COMPARISON OF AERIAL HYPERSPECTRAL AND MULTISPECTRAL IMAGERY: CASE STUDY OF NITROGEN MAPPING IN AUSTRALIAN COTTON

Anastasiia Volkova[a, b], Jon Baird[c], Irah Wajchman[b], Julian Guinane[a,b]

(a) University of Sydney, (b) FluroSat Pty Ltd, (c) Department of Primary Industries

ABSTRACT

With the commercialisation of hyperspectral sensing, a range of promising applications in precision agriculture, including nutrient mapping, are now becoming available to the research community and industry. An online workflow for calibration and analysis of the airborne multispectral and hyperspectral data including geo-rectification, derivation of vegetation indices and comparison with time series of the satellite data is being presented. The system is being demonstrated on a case study of nitrogen trials in Australian cotton conducted at Australian Cotton Research Institute (ACRI). The broadband and narrowband vegetation indices derived from hyperspectral imagery were compared with the satellite imagery from Sentinel 2B to assess the accuracy losses in mapping the variability of the field. The developed workflow has successfully been used for assessment of the quality and the suitability of the hyperspectral and multispectral aerial imagery for mapping in-field variability across the season. The comparison of the vegetation indices derived using source imagery from different sensors revealed the benefits of each of the imagery types and its potential for field variability mapping.

Index Terms— Airborne, hyperspectral, vegetation mapping, nitrogen, satellite imagery, cotton

1. INTRODUCTION

Cotton nitrogen use efficiency (NUE) is one the of the main levers of efficient fiber production. Although there is a body of research focusing on monitoring nitrogen stress with remote sensing (RS) technology; most of it has been conducted in controlled conditions where extensive testing and validation was performed. The most recent approaches to crop nitrogen mapping make use of multispectral (MS) imagery [1][2] but in the case of a crop with high nutrient requirements, like cotton, the vegetation indices (VIs) lose their relevance beyond the canopy closure phase due to saturation of broad spectral bands. The proposed crop canopy nitrogen mapping workflow developed into an online tool, FluroViewer, utilises airborne hyperspectral (HS) data alongside Sentinel 2A/B imagery to provide a viable and robust solution for near real-time nitrogen monitoring. The workflow includes data pre-processing, geo- and radiometric corrections, generation of relevant VIs, and detailed assessment of in-field variability. The tool allows users to evaluate the spectral responses on a per-trial or per-plot basis which is essential for adequate evaluation of the effects of the management techniques under controlled conditions. The results demonstrate the usefulness of the derived analytical insights and accessibility of the FluroViewer tool for the agricultural industry.

2. RELATED WORK

As stated in [1], traditional satellite imagery such as Landsat and SPOT has a long history of use in crop growth monitoring and to crop yield estimation over large geographic areas. The inherent weakness of the satellite imagery (limited spatial accuracy) has been recently addressed by increasing affordability of unmanned aerial systems (UAS, a.k.a. drones) carrying remote sensing payloads. Unmanned aerial system imagery has been utilised by [2] for the assessment of in-season cotton nitrogen status and lint yield prediction. In a series of 7 aerial surveys, it was found that vegetation indices Normalised Difference Red Edge (NDRE) and Simplified Crop Canopy Chlorophyll Index (SCCCI) have statistically significant correlation with the plant N% and N uptake during the early plant growth stages (first flower). Whilst other indices (NDVI) are more suitable for determining plant height and biomass. These indices have therefore been selected for the current study. Multispectral imagery acquired from a light aircraft over vineyards was compared to four Landsat scenes in [3]. The authors note that the imagery from the aircraft and satellite can be preferred to drone imagery, due to its guaranteed radiometric homogeneity and spectral consistency across the fields. By choosing the areas/pixels with known vegetation (excl. soil) to compare between aerial and satellite scenes, the authors have been able to achieve significant correlation of 0.85. The comparison of narrowband and broadband Normalised Difference Vegetation Index (NDVI) in [4] with plant measurements has found that higher correlation can be achieved when selecting a narrowband index, but failure to select the correct narrow bands may result in the opposite effect. The ground/soil interference effect was also mentioned by [5], when comparing vegetation indices derived from aerial multispectral data to ground hyperspectral data. Data with lower spatial resolution was found to be less accurate early in the season, when the crop canopy cover is sparse. In the current study the flight was performed at a later growth stage, which ensured sufficient crop canopy cover.

In [6], newer experimental indices were tested and compared to more traditional vegetation indices, such as those used in [2]. It confirmed the greater accuracy of chlorophyll based indices for crop health prediction at later stages of growth. The study forms the part of the basis of choosing the indices used in this research.

3. TRIAL SITE AND DATASET

3.1. Trial Setup

The multi-year cotton nitrogen application rate sensitivity trial has been set up in Norwood, NSW, Australia (2924'1.20"S, 14947'13.26"E) in 2016 with the goal of determining the potential yield gain from additional units of nitrogen applied pre-planting in September. The below image of the trial farm (Fig.1) has the head ditch at the right

and the tail drain to the left. A number of different treatments, i.e. 0, 37.5, 75, 112.5, 150 kg N/ha were established within the field with corresponding replications. Each treatment is trialled with and without dimethylpyrazole phosphate (DMPP), which is a nitrification inhibitor. Irrigation on each of the 12-meter-wide treatments (a plot) runs from head ditch to tail drain. The trial layout with sequence of nutrient applications and its three replications are shown in Fig. 1.

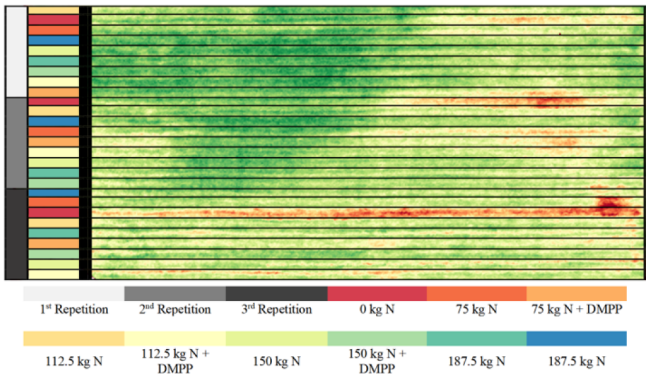

Fig. 1: Farm trial layout demonstrated on the NDRE index.

3.2. Satellite and airborne multispectral imagery

Collection of satellite imagery from Sentinel 2A/B satellites was performed automatically through the FluroViewer platform by supplying the field boundaries and date range for data collection. The satellite data, as it will be seen later in result section 5, provides consistency to the time series and functions as a baseline against which all other imagery sources are calibrated. When referring to imagery in this paper, it is understood that the multi-/hyperspectral bands extracted from the raw product (captured from satellite or plane) are used to derive the vegetation indices that are the key focus of the analysis. Satellite imagery, although consistent and frequent, is often lacking the level of detail required to identify individual trials in the field as they are only 12 m wide whilst the resolution of satellite bands is 10-20-60 m for Sentinel 2A/B. Therefore, it is required to collect aerial imagery to achieve higher spatial resolution (0.75-1.5 m). We have collected three aerial datasets for comparison, two using a multispectral camera and one using a hyperspectral system (see Fig. 3). Both camera systems were flown on a fixed-wing airplane at an altitude of about 1,200 m. The multispectral images were taken on 12.12.17, and 18.01.18 using a High Resolution Airborne Multispectral Sensor (HiRAMS) System built by SpecTerra Services Pty Ltd (Leederville 6007, WA, Australia).

3.3. Airborne hyperspectral imagery

To demonstrate the capabilities of hyperspectral imaging and provide detailed data for the research trial analysis, a remote sensing dataset was collected with the airborne hyperspectral imaging system Resonon Pika L [7]. It is a pushbroom-type camera, triggered by a flight computer running on an Intel NUC, integrated with onboard GNSS and IMU. The number of spectral bands can be set to 150 and 281 within the spectral range of 380-1020 nm (min - 2.1 nm bands). The imager has 900 spatial channels and a frame rate of 249 fps. The dataset was acquired during the second flight on 15.02.18 at the altitude of 1,200 m.

3.4. Low-altitude (drone) airborne multispectral data

Originally the aerial imagery captured with a Micasense RedEdge M sensor was planned to be added to the dataset. The flight was conducted on 30th January 2018 at an altitude of about 100 m AGL. The resulting ortho-mosaic was complete (shown in Fig. 2) but the changes in reflectance values from image row to image row (due to the variation in the Sun angle when drone was changing the flight direction) were equivalent on the order of magnitude to variability in the aerial image. The lack of adequate inter-frame radiometric calibration prevented us from using the Micasense dataset in the present study.

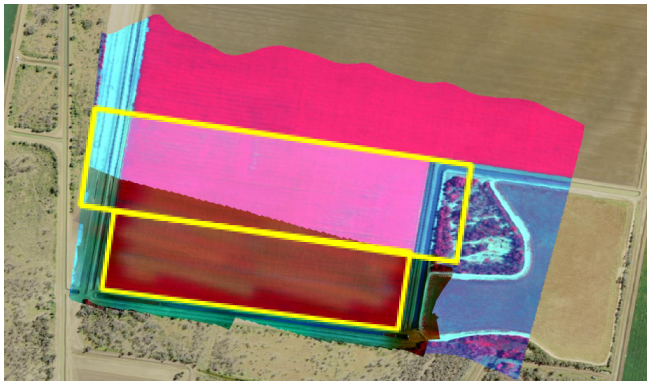

Fig. 2: (bottom up) False colour image taken using drone-mounted MicaSense RedEdgeM in red, airplane-mounted HiRAMS in light pink and Resonon Pika L in bright pink. Outline of the trial area shown in yellow.

4. METHODOLOGY

4.1. Pre-processing and accuracy assessment

The raw linescan data first needs to be binned and brought to a suitable resolution (1.5 m GSD) using the Resonon Spectronon software package. The resulting hypercubes are automatically geo-referenced on a line-per-line basis. The automatic geo-registration procedure heavily depends on the accuracy of the onboard GNSS solution, which when inaccurate can result in spatial warping. This is due to differences in relative error at each scanline of the sensor. The upper error bound on the spatial accuracy of the GNSS solution supplied with the system in Australian conditions according to the supplier is 15m. This is naturally too coarse for the application in question (the plots are only 12 m wide) and required further geo-correction. This step has been historically performed by a system operator but can also be replaced by novel automatic feature matching algorithms.

4.2. Generation of vegetation indices (VIs)

To perform time-series analysis on the vegetation indices the user needs to access all the indices and related information in one location, hence the airborne imagery needs to be imported into the systems alongside airborne and satellite multispectral imagery. We propose to utilise the hyperspectral imagery in two ways: 1) derive the vegetation indices available for fast viewing and interaction, and 2) perform analysis of the full spectral signatures related to different trial areas.

To perform the first type of analysis, a range of specific narrowband and broadband vegetation indices mimicking the Sentinel 2A/2B satellite bands are generated in an automatic fashion. Instead of deriving the full range of vegetation indices used in remote sensing [2][6], we are concentrating on the indices that have shown statistically significant correlation in previous studies, namely NDVI, NDRE, SCCCI.

$$\mathrm{NDVI} = \mathrm{NIR} - \mathrm{RED}/\mathrm{NIR} + \mathrm{RED}$$

$$\mathrm{NDRE} = \mathrm{NIR} - \mathrm{REDGE}/\mathrm{NIR} + \mathrm{REDGE}$$

$$\mathrm{SCCCI} = \mathrm{NDRE}/\mathrm{NDVI}$$

Table 1: Hyperspectral broad bands (HiRAMS equivalent)

Band	min (nm)	max (nm)
RED	665	685
REDGE	700	720
NIR	770	790

Table 2: Hyperspectral narrow bands (generated)

Band	centre (nm)	bandwidth (nm)
RED	675.34	4.3
REDGE	709.52	4.3
NIR	778.48	4.3

Table 3: Multispectral MicaSense RedEdge-M bands (collected)

Band	centre (nm)	bandwidth (nm)
RED	668	10
REDGE	717	10
NIR	840	40

4.3. Radiometric calibration of the imagery

Once the produced vegetation indices are generated from aerial hyperspectral and aerial/satellite multispectral imagery, they are automatically overlaid over a global map in a common coordinate reference system. To combine imagery from different sources into a consistent time series for change analysis, it is necessary to perform radiometric calibration on the images, bringing them to a common baseline. For large-scale projects such as cross-calibration of satellite sensors, large spectrally invariant targets such as sand dunes or salt lakes are normally used [8]. In a precision agriculture scenario, where the data is being collected for the purpose of monitoring specific cropping areas, it is necessary to find an alternative to commonly-used large invariant targets. In our case, we are utilizing the approach of cross-calibrating the aerial imagery band-by-band by relative to invariant non-vegetative regions in the imagery. This operation is performed automatically by masking out the vegetation using thresholding of the NDVI index and finding the areas with least variation to use as spectral control points.

4.4. Performing the analysis on VIs

The series of vegetation indices brought in alignment using the geo- and radiometric correction steps described above, were analysed by selecting a number of points of interest and comparing the performance of the crop in those areas over time. The ability to combine the regularly-captured satellite imagery with airborne datasets allows the users to select from a wide range of data and spatial resolutions the best fit for the purpose of their specific applications. Although the satellite imagery lacks the detailed resolution of the airborne data, it allows the users to track large-scale changes and overall patterns prevalent in the fields. Complimentary power of the aerial imagery is in its detail allowing the precision required for the applications such as the monitoring and quantitative analysis of the agronomic trials. To further improve the precision of the generated VIs and extract the full value of the spatial information about the in-field variability, the VIs can be further calibrated using laboratory tissue testing allowing to quantify the nitrogen sensitivity of the cotton crop in agronomic terms.

5. RESULTS AND ANALYSIS

5.1. Time-series analysis on cross-calibrated index layers

The benefit of VIs derived from airborne multi-/hyperspectral imagery can be seen when considered in context of the VIs generated across the season (Fig. 3-4). At the start of the season, the SCCCI (Fig.3, left) shows the variability in the field, which disappears as the index saturates towards the crop maturity phase (Fig. 3 right). Narrowband hyperspectral analysis (Fig.4), on the other hand, captures a sufficient level of variability even late in the season which allows to track in-field and cross-trial changes at a high level of detail. The image-based analysis includes time series, histogram, and full spectrum analysis (FSA) as presented in section 5.3.

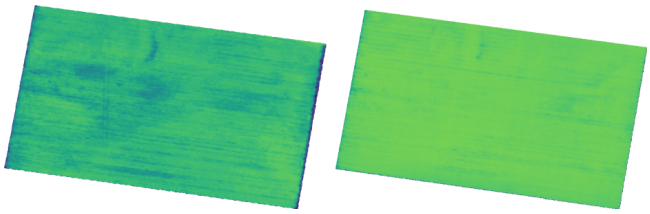

Fig. 3: SCCCI derived from HiRAMS image from 12.12.17 (left) showing variability compared to 18.01.18 (right).

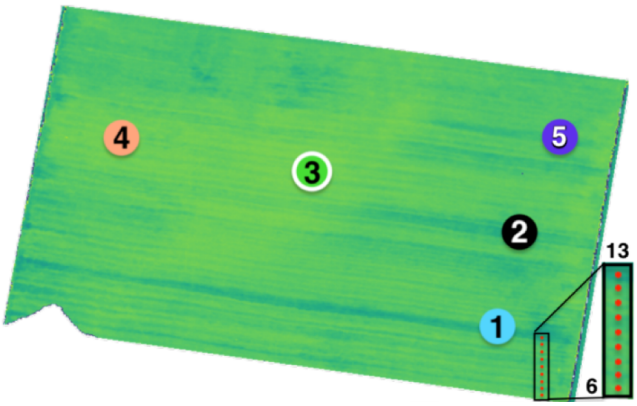

Fig. 4: Hyperspectral SCCCI (narrowband) from 15.02.18 with sparse (1-5) and dense (6-13) points chosen for FSA in Section 5.3.

The time series analysis (Fig. 5) of first order derived indices such as NDVI demonstrates predictable growth curves with aerial

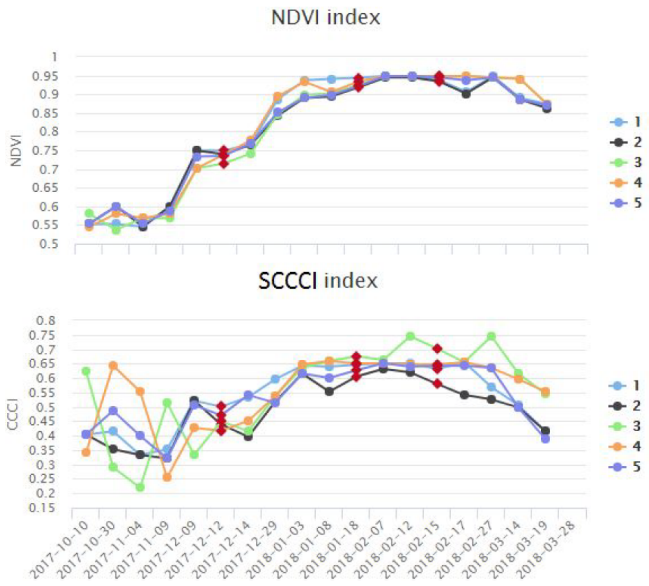

Fig. 5: NDVI and SCCCI trends for 5 points in Fig. 4.

imagery values (marked by red diamonds) appropriately fitting within the range of the data in the trend. The SCCCI index, having been derived from the other two indices early in season, is subjected to noise due to high soil reflectance values obfuscating the NDRE layer until the crop develops significant canopy cover to be clearly differentiated from the soil signal. The value of the SCCCI analysis is in its ability to highlight the subtle changes within the field as can be seen in Fig. 5, where all the aerial imagery points (red diamonds) are clearly separable.

5.2. Index comparison

To provide an objective comparison of the various spectral properties of the cameras, demonstrate the effect that the platform and the crop growth stage can have on the variability within a vegetation index, the SCCCI indices were presented using the same linear colour-map show below.

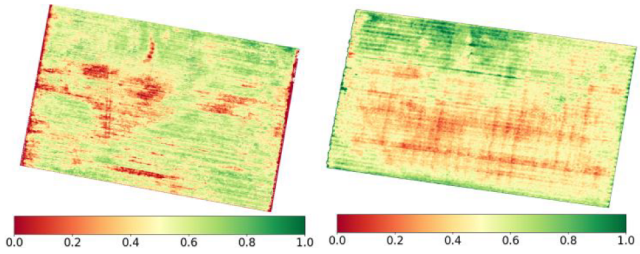

Fig. 6: HiRAMS SCCCI 12.12.17 (left), 18.1.18 (right).

When comparing the distribution of the values of each of the indices on the histogram, it is evident that the values of each of the histograms move to saturation (towards 1) as the crop grows and becomes more reflective/absorptive in teh bands used to calculate the index. It is notable however, that the HS histogram demonstrates wider spread of values likely caused by higher spectral sensitivity of the sensor, which may act a significant advantage to precision

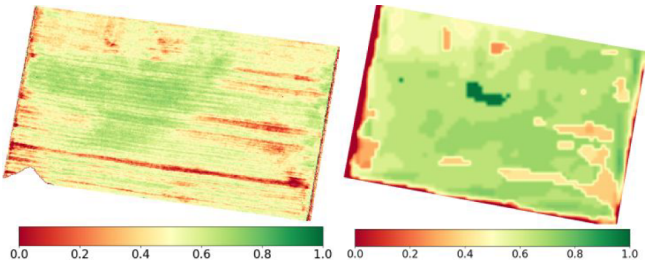

Fig. 7: HS narrowband SCCCI from 15.02.18 ((left) and Sentinel 2B-derived SCCCI from 17.02.18 (right).

agriculture applications and agronomic trials in particular. One of the important outcomes of the study is proof that hyperspectral imagery can be useful to differentiate variability in the field even late in season, when multispectral imagery is saturated and becomes insensitive to variations. This can be particularly useful for the end-of-season crop biomass estimation needed for yield prediction.

The effect that the satellite image has when serving as a source of vegetation index data is demonstrated with the histogram comparison of a multispectral satellite image and hyperspectral aerial image acquired within a two day period (see Fig 8). SCCCI images show a much wider variance of values in the hyperspectral images when compared with the Sentinel 2 images. The frequencies of the satellite-based MS SCCCI index are concentrated around few reflectance values and biased towards lower end of the reflectance values. When used for assessment of the fertilisation strategy these effects may result in under- or over-estimation of the crop stress and. hence, required amount of the fertiliser. The satellite imagery, as stated earlier can still be a useful scouting tool by guiding the user to the areas that require more attention on the field. For the precision agriculture perspective, the spatial resolution of the imagery needs to be on the order of 5m in all used bands to be representative of the more detailed changes.

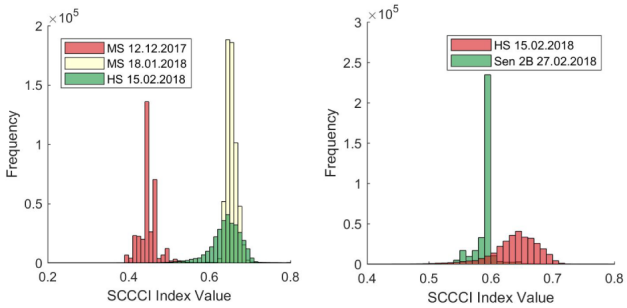

Fig. 8: Comparison of MS and HS SCCCI index values (left). Comparison of aerial HS SCCCI with satellite-based MS SCCCI from 15.02.18 (right)

5.3. Full spectrum analysis

To further investigate the variability of the hyperspectral signal for each of the various targets present in the imagery, the points 1-6 were picked in representative areas of the hyperspectral cube representing road (4), trees (3), grasslands (6) and vegetation (1,2,5)(Fig. 10). Full spectrum analysis (Fig. 9) shows clear separation between the

classes chosen for comparison. The pixels of the road class (4) are most likely causing the saturation effect due to high reflectivity.

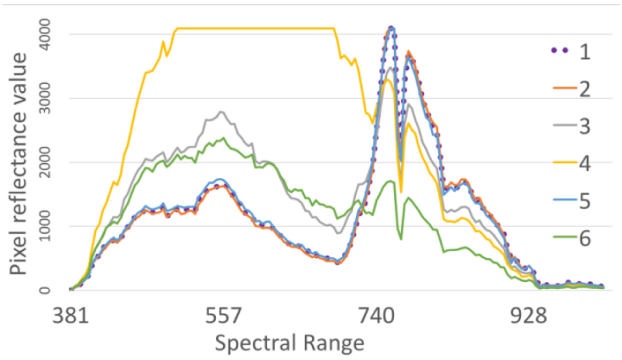

Fig. 9: Spectral signatures of the points 1-6 in Fig.10.

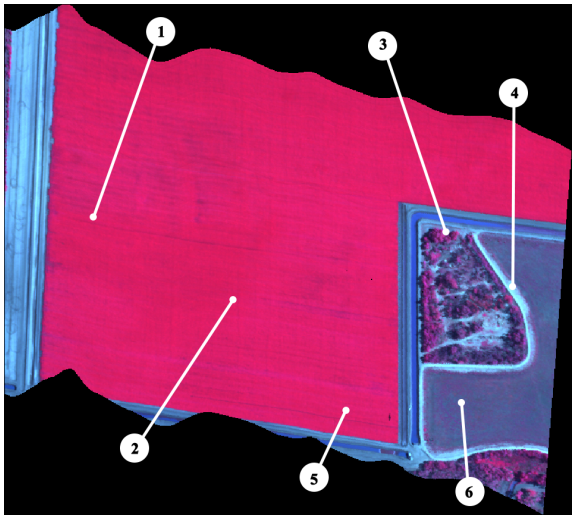

Fig. 10: Representative areas of the hyperspectral cube representing road (4), trees (3), grasslands (6) and vegetation (1,2,5) used in full spectrum analysis.

For the purposes of evaluating the sensitivity of the hyperspectral imagery to parameters driving the agronomic trials in cotton (various nitrogen rates) the points 6-13 across the trial set up centered approximately in each of the trials plots with 12 m separation starting from the bottom of the image (as shown in Fig.4) were chosen. The spectral signatures of each of the points centered on a trial plot can be seen in Fig. 11. The close up look at the peaks in green and infrared allow us to identify the potential wavelength which would be most appropriate for selective narrowband multispectral analysis. The graph demonstrates the subtle variability that requires accurate radiometric calibration of the imagery for reliable separation of the trials.

6. FUTURE WORK

The time-series of vegetation indices presented in this paper derived from different spectral sources will contribute to crop canopy nitrogen status mapping once the tissue sampling results are returned

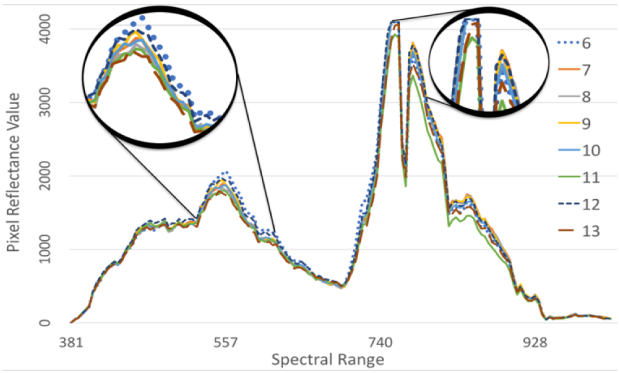

Fig. 11: Spectral signatures of the points 6-13 in Fig.4

from the laboratory. The vegetation indices will be combined with the irrigation data to enhance the presented analysis and assess the potential of the demonstrated vegetation indices to predict yield variability early in season - when intervention is still possible. The tissue sampling results and yield maps for the trial will become available within the time allocated for approval of this paper, which will enable the authors to complete extensive analysis on the enhanced dataset.

7. REFERENCES

[1] C. Yang, J. H. Everitt, Q. Du, B. Luo, and J. Chanussot, "Using high-resolution airborne and satellite imagery to assess crop growth and yield variability for precision agriculture," *Proceedings of the IEEE*, vol. 101, no. 3, pp. 582–592, March 2013.

[2] Carlos Ballester, John Hornbuckle, James Brinkhoff, John Smith, and Wendy Quayle, "Assessment of in-season cotton nitrogen status and lint yield prediction from unmanned aerial system imagery," *Remote Sensing*, vol. 9, no. 11, 2017.

[3] E. Borgogno-Mondino, A. Lessio, L. Tarricone, V. Novello, and L. de Palma, "A comparison between multispectral aerial and satellite imagery in precision viticulture," *Precision Agriculture*, vol. 19, no. 2, pp. 195–217, Apr 2018.

[4] Prasad S Thenkabail, Ronald B Smith, and Eddy De Pauw, "Hyperspectral vegetation indices and their relationships with agricultural crop characteristics," *Remote Sensing of Environment*, vol. 71, no. 2, pp. 158 – 182, 2000.

[5] Huihui Zhang, Yubin Lan, Ronald Lacey, W. C. Hoffmann, and Yanbo Huang, "Analysis of vegetation indices derived from aerial multispectral and ground hyperspectral data," *International Journal of Agricultural and Biological Engineering*, vol. 2, pp. 33–40, September 2009.

[6] Pablo Zarco-Tejada, Michael Whiting, and Susan Ustin, "Temporal and spatial relationships between within-field yield variability in cotton and high-spatial hyperspectral remote sensing imagery," vol. 97, 05 2005.

[7] Resonon, "Pika l - vnir hyperspectral imaging camera," .

[8] Sentinel-2 PDGS Project Team, "Sentinel-2 calibration and validation plan for the operational phase," Tech. Rep., European Space Agency, 12 2014.